Acta Crystallographica Section D
Biological Crystallography
ISSN 0907-4449

Preferential selection of isomer binding from chiral mixtures: alternate binding modes observed for the *E* and *Z* isomers of a series of 5-substituted 2,4-diaminofuro[2,3-*d*]pyrimidines as ternary complexes with NADPH and human dihydrofolate reductase

Vivian Cody,[a,b]* Jennifer Piraino,[a] Jim Pace,[a] Wei Li[c] and Aleem Gangjee[c]

[a]Structural Biology Department, Hauptman–Woodward Medical Research Institute, 700 Ellicott Street, Buffalo, NY 14203, USA, [b]University of Buffalo, 700 Ellicott Street, Buffalo, NY 14203, USA, and [c]Graduate Division, Medicinal Chemistry, Duquesne University, Pittsburgh, PA 15213, USA

Correspondence e-mail: cody@hwi.buffalo.edu

Received 9 August 2010
Accepted 6 September 2010

PDB References: hDHFR ternary complexes, 3nxo; 3nxr; 3nxt; 3nxv; 3nxx; 3nxy.

The crystal structures of six human dihydrofolate reductase (hDHFR) ternary complexes with NADPH and a series of mixed *E*/*Z* isomers of 5-substituted 5-[2-(2-methoxyphenyl)-prop-1-en-1-yl]furo[2,3-*d*]pyrimidine-2,4-diamines substituted at the C9 position with propyl, isopropyl, cyclopropyl, butyl, isobutyl and *sec*-butyl (*E*2–*E*7, *Z*3) were determined and the results were compared with the resolved *E* and *Z* isomers of the C9-methyl parent compound. The configuration of all of the inhibitors, save one, was observed as the *E* isomer, in which the binding of the furopyrimidine ring is flipped such that the 4-amino group binds in the 4-oxo site of folate. The *Z*3 isomer of the C9-isopropyl analog has the normal 2,4-diaminopyrimidine ring binding geometry, with the furo oxygen near Glu30 and the 4-amino group interacting near the cofactor nicotinamide ring. Electron-density maps for these structures revealed the binding of only one isomer to hDHFR, despite the fact that chiral mixtures (*E*:*Z* ratios of 2:1, 3:1 and 3:2) of the inhibitors were incubated with hDHFR prior to crystallization. Superposition of the hDHFR complexes with *E*2 and *Z*3 shows that the 2′-methoxyphenyl ring of *E*2 is perpendicular to that of *Z*3. The most potent inhibitor in this series is the isopropyl analog *Z*3 and the least potent is the isobutyl analog *E*6, consistent with data that show that the *Z* isomer makes the most favorable interactions with the active-site residues. The isobutyl moiety of *E*6 is observed in two orientations and the resultant steric crowding of the *E*6 analog is consistent with its weaker activity. The alternative binding modes observed for the furopyrimidine ring in these *E*/*Z* isomers suggest that new templates can be designed to probe these binding regions of the DHFR active site.

1. Introduction

2,4-Diamino-5-substituted furo[2,3-*d*]pyrimidines, by virtue of their structural analogy to the anticancer agent trimetrexate, were designed as inhibitors of human dihydrofolate reductase (hDHFR) with the potential to be used as antitumor agents (Gangjee *et al.*, 2005). Structure–activity correlations for the inhibition of hDHFR by a series of chirally mixed *E* or *Z* isomers of 5-substituted 5-[2-(2-methoxyphenyl)-prop-1-en-1-yl]furo[2,3-*d*]pyrimidine-2,4-diamines revealed that extension of the 9-methyl parent compound resulted in moderately active inhibitors of hDHFR and that the C9-methyl analog *Z*1 (Fig. 1) was the most potent inhibitor (K_i = 0.5 μ*M*), while the isobutyl analog *E*6 (Fig. 1) was the least potent (K_i = 11.0 μ*M*)

Table 1
Crystal properties and refinement statistics for the series of substituted *E*/*Z* isomers of furopyrimidines shown in Fig. 1 bound to hDHFR.

Values in parentheses are for the outer shell.

Compound	*Z*3	*E*2	*E*4	*E*5	*E*6	*E*7
PDB code	3nxo	3nxr	3nxt	3nxv	3nxx	3nxy
Space group	*H*3	*H*3	*H*3	*H*3	*H*3	*H*3
Unit-cell parameters (Å)						
a	84.15	84.50	84.42	84.00	84.35	84.42
b	84.15	84.50	84.42	84.00	84.35	84.42
c	77.97	78.13	77.55	78.27	77.65	77.35
Beamline	SSRL 9-2	SSRL 9-2	SSRL 9-2	R-AXIS IV	SSRL 9-2	SSRL 9-2
Resolution (Å)	1.35 (1.42)	1.35 (1.42)	1.70 (1.80)	1.90 (2.00)	1.35 (1.42)	1.80 (1.90)
Wavelength (Å)	0.975	0.975	0.975	1.5417	0.975	0.975
R_{merge}	0.068 (0.5)	0.118 (0.30)	0.042 (0.10)	0.055 (0.16)	0.061 (0.40)	0.27 (0.34)
Completeness (%)	99.9 (100.0)	100.0 (100.0)	99.9 (100.0)	99.8 (98.6)	100.0 (100.0)	100.0 (100.0)
Observed reflections	391472 (54341)	405383 (57028)	211460 (30083)	56728 (7223)	401743 (55786)	107015 (15492)
Unique reflections	45197 (6605)	45693 (6687)	22685 (3353)	16181 (234)	45270 (6622)	19048 (2789)
$\langle I/\sigma(I)\rangle$	18.9 (4.4)	12.5 (0.9)	34.7 (16.5)	14.4 (6.0)	21.4 (4.7)	5.2 (0.6)
Multiplicity	8.7 (8.2)	8.9 (8.5)	9.3 (9.0)	3.5 (3.1)	8.9 (8.4)	5.6 (5.6)
Reflections used	42917	43214	21522	15365	42985	15398
R factor	0.19	0.20	0.18	0.19	0.18	0.21
R_{free}	0.21	0.22	0.22	0.24	0.21	0.27
Total protein atoms	1803	1814	1835	1812	1849	1860
Total water atoms	165	184	125	92	237	55
Average *B* factor (Å^2)	16.3	21.6	15.1	16.5	16.5	24.6
Error in Luzzati plot	0.16	0.18	0.17	0.20	0.15	0.25
R.m.s. deviation from ideal						
Bond lengths (Å)	0.034	0.031	0.028	0.025	0.034	0.022
Bond angles (°)	2.79	2.77	2.65	2.35	2.92	2.10
Ramachandran plot						
Most favored	97.3	98.4	98.4	98.4	96.7	97.3
Additional allowed	1.6	1.6	1.6	1.6	3.3	2.7
Disallowed	1.1	0.0	0.0	0.0	0.0	0.0

for this series of chirally mixed analogs (Gangjee *et al.*, 2009). The *E* isomer is defined as having the 2′-methoxyphenyl ring *trans* to the furopyrimidine ring, while the *Z* isomer is defined as having these groups *cis* to each other.

Previous structural studies of the chirally resolved *Z* and *E* isomers of the C9-methyl parent compound (Fig. 1) revealed that the *Z* isomer fitted into the hDHFR active site in the normal 2,4-diaminofuropyrimidine ring orientation of antifolates, whereas the *E* isomer could not easily be accommodated unless the 2,4-diaminofuropyrimidine ring was flipped such that Glu30 interacted with the 2-amino group and N3 of the pyrimidine ring and the furo oxygen occupied the N4 amino position (Gangjee *et al.*, 2005, 2009).

To further explore the factors that influence diaminopyrimidine ring flipping in the binding of furo[2,3-*d*]pyrimidine analogs to DHFR, structural data were determined for the series of mixed *E*/*Z* isomers of C9-substituted furo[2,3-*d*]-pyrimidines where the C9 substituent is propyl, isopropyl, cyclopropyl, butyl, isobutyl and *sec*-butyl (Fig. 1). These data are compared with the structures of the resolved *E* and *Z* isomers of the parent C9-methyl diaminofuropyrimidine *E*1 and *Z*1 determined as ternary complexes with NADPH and human and mouse DHFR (Gangjee *et al.*, 2009; Cody *et al.*, 2009). The compounds shown in Fig. 1 are defined by a number such that propyl is 2, isopropyl is 3 using the numbering scheme as described by Gangjee *et al.* (2009); furthermore, the isomer observed in the resulting crystal structure is also indicated using the *E*/*Z* notation, resulting in compounds *E*2, *Z*3 *etc*.

2. Methods

2.1. Crystallization

Recombinant hDHFR was expressed and purified as described previously (Gangjee *et al.*, 2009). The protein was washed in a Centricon-10 with 100 m*M* K_2HPO_4 buffer pH 6.9 and concentrated to 8.2 mg ml^{-1}. Prior to crystallization using the hanging-drop vapor-diffusion method, the protein was incubated for 1 h on ice with a 10:1 molar 100 m*M* excess of NADPH and the inhibitors 2–7 (Fig. 1). Protein droplets contained K_2HPO_4 pH 6.9 with 30% saturated ammonium sulfate and 3%(*v*/*v*) ethanol. Crystals grew over several days and were rhombohedral, belonging to space group *H*3, and diffracted to between 1.9 and 1.4 Å resolution for the six complexes. Data for all but one complex were collected on beamline 9-2 at the Stanford Synchrotron Radiation Laboratory using the remote-access system (Cohen *et al.*, 2002; González *et al.*, 2008; McPhillips *et al.*, 2002). Data for the C9-butyl *E*5 analog complex were collected at liquid-nitrogen temperature on a Rigaku R-AXIS IV imaging-plate system with MaxFlux optics and the data were processed using both *DENZO* (Otwinowski & Minor, 1997) and *MOSFLM* (Collaborative Computational Project, Number 4, 1994). Diffraction statistics are shown in Table 1 for all complexes.

2.2. Structure solution

The structures were solved by molecular-replacement methods using the coordinates of hDHFR (PDB code 1u72; Cody *et al.*, 2005) in the program *MOLREP* (Collaborative

Table 2
Bridge torsion angles (°) for *E*/*Z* isomers bound to human DHFR (hDHFR) or mouse DHFR (mDHFR).

Inhibitor	C6—C5—C8—C9	C5—C8—C9—C1′	C8—C9—C1′—C2′	C5—C8—C9—C91	C8—C9—C91—C92	Furopyrimidine ring orientation
mDHFR *Z*1†	8.3	−9.7	−88.1	176.4	—	Normal‡
hDHFR *Z*1§	27.0	−8.3	−88.2	168.0	—	Normal
mDHFR *E*1†	−16.2	−171.5	−89.7	10.8	—	Flipped‡
hDHFR *Z*3	25.6	−8.5	−81.9	175.2	94.3	Normal
hDHFR *E*2	−101.8	−166.9	96.6	7.5	110.5	Flipped
hDHFR *E*4	0.5	−170.0	−83.0	25.3	159.9	Flipped
hDHFR *E*5	−81.2	−175.6	96.3	−2.6	117.2	Flipped
hDHFR *E*6	−66.2	−161.5	86.3			Flipped
Conformer *C*				0.2	−127.0	
Conformer *B*				46.9	101.7	
hDHFR *E*7	−74.9	−178.9	91.5	7.6	95.4	Flipped

† Gangjee *et al.* (2009). ‡ Normal antifolate binding is that in which Glu30 interacts with the 2-NH_2 and N1 of the diaminofuropyrimidine ring; flipped binding is that in which Glu30 interacts with the 4-NH_2 and N3 of the diaminofuropyrimidine ring. § Cody *et al.* (2009).

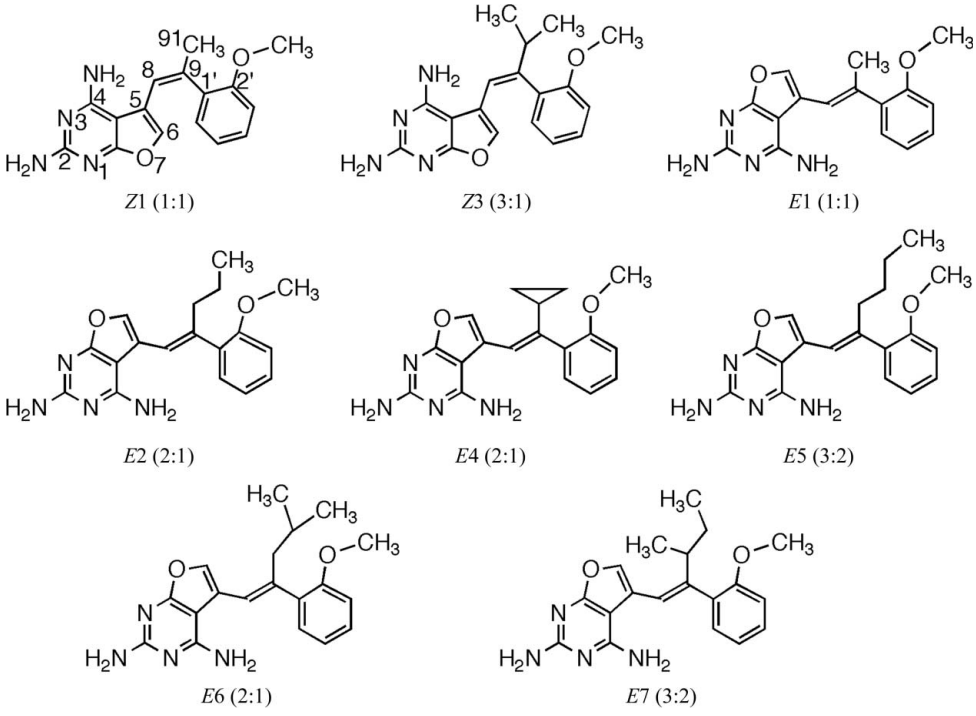

Figure 1
Schematic representation of the 2,4-diaminofuro-[2,3-*d*]pyrimidines under study. The *E* isomer is defined as having the 2′-methoxyphenyl ring *trans* to the furopyrimidine ring, while the *Z* isomer is defined as having these groups *cis* to each other. In these structures, the 2′-methoxyphenyl ring occupies the same position in the active site, while the furopyrimidine ring flips its orientation from the normal antifolate-binding mode. The values in parentheses refer to the *E*:*Z* ratio of the chiral isomers. Compound numbers are defined as listed in Gangjee *et al.* (2009).

Computational Project, Number 4, 1994). Inspection of the resulting difference electron-density maps was made using the program *Coot* (Emsley & Cowtan, 2004) running on a Mac G5 workstation and revealed density for a ternary complex in all cases. To monitor the refinement, a random subset of all reflections was set aside for the calculation of $R_{\rm free}$ (5%). The models and parameter files for the inhibitors were prepared using the *PRODGR*2 server website at the University of Dundee (http://davapc1.bioch.dundee.ac.uk/programs/prodrg; Schüttelkopf & van Aalten, 2004). Refinement was carried out using the program *REFMAC*5 from the *CCP*4 suite of programs (Collaborative Computational Project, Number 4, 1994). The Ramachandran conformational parameters from the last cycle of refinement generated by *RAMPAGE* (Lovell *et al.*, 2002) showed that more than 98% of the residues in these hDHFR complexes have the most favored conformation and none are in disallowed regions (Table 1). Coordinates for the structures have been deposited in the Protein Data Bank (PDB codes 3nxo, 3nxr, 3nxt, 3nxv, 3nxx and 3nxy).

3. Results

Structure determination of six ternary complexes of hDHFR with NADPH and the chirally mixed series of 5-substituted 5-[2-(2-methoxyphenyl)-prop-1-en-1-yl]-furo[2,3-*d*]pyrimidine-2,4-diamine inhibitors with propyl, isopropyl, cyclopropyl, butyl, isobutyl and *sec*-butyl substitutions at C9 (Fig. 1) reveals that in all cases only one isomer of the chiral mixture is observed to bind in the hDHFR active site, regardless of the isomer ratio present in the mixture upon crystallization (Fig. 2). Furthermore, of the six structures only the isopropyl analog (*Z*3; Fig. 1; Table 2) shows the normal antifolate-binding mode for the furopyrimidine ring in which the 2-amino group and N1 interact *via* hydrogen bonds to Glu30, similar to that of methotrexate (Cody *et al.*, 2005; Cody & Schwalbe, 2006). In this orientation the 4-amino group of the furopyrimidine ring interacts with the backbone functional groups of Ile7 and Val115, the hydroxyl of Tyr121 and the nicotinamide carboxamide group of NADPH (Fig. 2*a*). In the other five complexes the furopyrimidine ring binds in a flipped orientation such that the 4-amino group and N3 interact with Glu30 and the furo oxygen occupies the binding site of the 4-amino group observed in the antifolate orientation (Fig. 2*b*). The furo O atom accepts a hydrogen bond from the NH_2 of the nicotinamide of NADPH and makes weak contacts *via* the lone pair of electrons on the oxygen to the carbonyl of Ile7 and to the functional groups of Val115 and Tyr121.

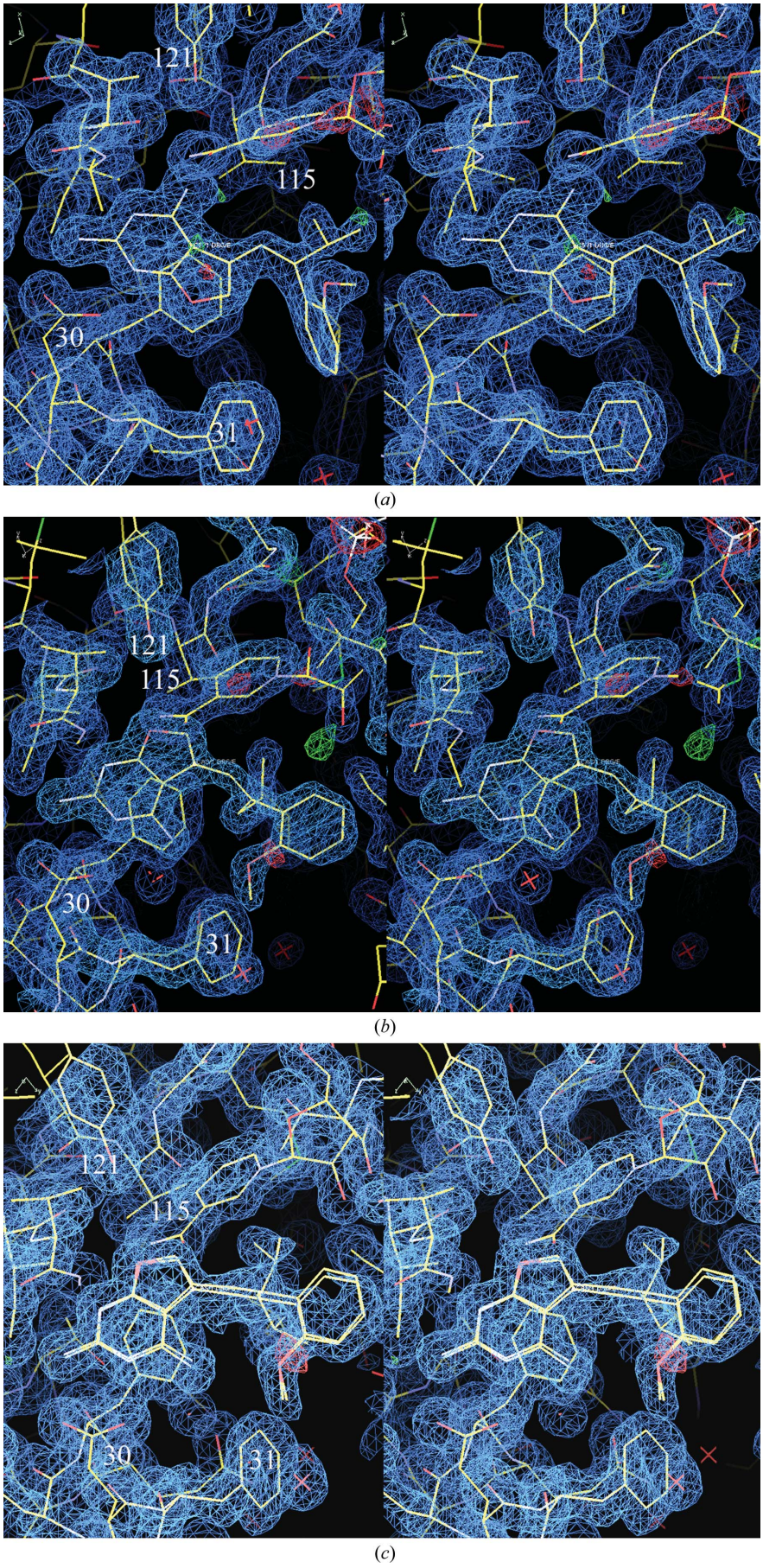

The structure of the C9-isopropyl analog (*Z*3; Fig. 1) shows that the *Z* isomer was selected from the 2:1 mixture of *E*/*Z* isomers incubated during crystallization. The *Z* isomer places the 2-methoxyphenyl ring *cis* to the furopyrimidine ring, as indicated by the torsion angle about the C8═C9 double bond (Table 2) and as illustrated in Fig. 2(*a*). In this orientation, the C9-isopropyl group makes van der Waals contact with the methyl group of Thr56 (3.5 Å; Table 3). On the other hand, the structures of the other five 9-substituted analogs (Fig. 1) reveal a binding preference for the *E* isomer, which places the 2′-methoxyphenyl ring *trans* to the furopyrimidine ring as indicated by the torsion angle about the C8═C9 bond (Table 2) and illustrated in Fig. 2(*b*). The remaining torsion angles described in Table 2 illustrate the consistency of the 2′-methoxyphenyl conformation in this series (Fig. 3). This figure also shows that Glu30 does not undergo a rotameric change in its conformation when bound to these inhibitors.

The furo oxygen of analogs *E*2 and *E*4–*E*7 make weak contacts to Ile7, Val115, Tyr121 and the nicotinamide of NADPH. In these analogs, the closest contact of the 2′-methoxy methyl group is to Leu22 (∼3.6 Å). The isopropyl group of *Z*3

Figure 2
(*a*) View of the $2F_o - F_c$ difference electron-density map for hDHFR–NADPH–*Z*3 contoured at 1.1σ (blue). The red crosses represent water molecules. These data clearly show a ternary complex with the inhibitor *Z*3 binding in the normal antifolate orientation with N1 and the 2-amino group interacting with Glu30. The configuration about the propenyl double bond is *Z*, with the 2′-methoxyphenyl ring *cis* to the furopyrimidine ring. (*b*). View of the $2F_o - F_c$ difference electron-density map for hDHFR–NADPH–*E*2 contoured at 1.4σ (blue). These data clearly show a ternary complex with the inhibitor *E*2 bound with a 'flipped' furopyrimidine orientation with the furo oxygen occupying the position of the 4-amino group of the antifolate. The configuration about the propenyl double bond is *E*, with the 2′-methoxyphenyl ring *trans* to the furopyrimidine ring. (*c*) View of the $2F_o - F_c$ difference electron-density map for hDHFR–NADPH–*E*6 contoured at 0.9σ (blue). These data clearly show a ternary complex with the inhibitor *E*6 bound with a 'flipped' furopyrimidine orientation with the furo oxygen occupying the position of the 4-amino group of the antifolate. Note the disorder in the C9-isobutyl side chain. The configuration about the propenyl double bond is *E*, with the 2′-methoxyphenyl ring *trans* to the furopyrimidine ring.

makes close hydrophobic contacts with the side chains of residues Ile60 and Val115, as well as with Thr56 (Table 3). The contacts for *Z*3 are the most favorable among this series of analogs, followed by the cyclopropyl (*E*4) and isobutyl (*E*6) analogs.

Analysis of the isobutyl analog *E*6 (Fig. 1) reveals that the isobutyl group is statistically disordered with 50% occupancy (Fig. 2*c*). One conformer (*C*) has torsion angles similar to those of the other C9-substituted analogs, whereas the other conformer (*B*) is twisted away and is about halfway between the *cis* and *trans* orientations (Table 2). Inspection of the environment around the isobutyl group shows that conformer *B* makes contact with Leu22, Phe31 and Ile60, while the *C* conformer makes contacts with Thr56, Ile60 and Val115. The C9-butyl (*E*5; Fig. 1) substituent has an extended conformation with one *gauche* torsion angle that folds the butyl group such that it does not extend beyond the other C9 substituents (Fig. 3). The terminal carbon of the group makes contacts with Thr56, Ile60, Leu67 and Phe34 that are similar to those of the isobutyl and *sec*-butyl analogs (Table 3).

Table 3
Intermolecular interactions of the C9-substituents (terminal atom) in the *E*/*Z* isomers with the hydrophobic residues in the active site of DHFR.

	Distance (Å) between inhibitor C9 and			
	Ile60 CD1	Ile67 CD1	Val115 CG2	Thr56 CD1
mDHFR *E*1	4.7	5.0	4.4	3.9
mDHFR *Z*1	3.9	4.3	3.7	3.6
hDHFR *Z*1	3.9	4.7	4.4	3.6
hDHFR *Z*3	3.6	4.5	3.4	3.5
hDHFR *E*2	4.2	4.3	4.0	4.1
hDHFR *E*4	3.5	4.5	4.0	3.5
hDHFR *E*5	4.2	3.9	3.5	3.8
hDHFR *E*6	3.9	4.5	3.5	3.4
hDHFR *E*7	4.5	4.4	3.5	3.9

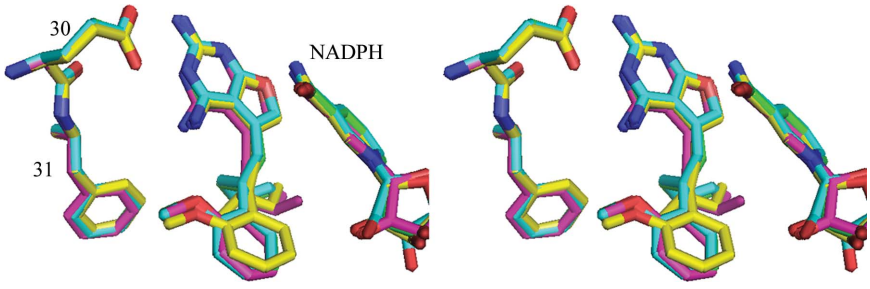

Figure 3
Stereo comparison of the binding of *E*2 (green), *E*5 (cyan), *E*6 (violet) and *E*7 (yellow) in hDHFR ternary complexes with NADPH. The active-site residues Glu30 and Phe31 are shown. Note that the 2′-methoxyphenyl ring binds in the same orientation in each of these complexes. This figure was drawn with *PyMOL* (DeLano, 2002).

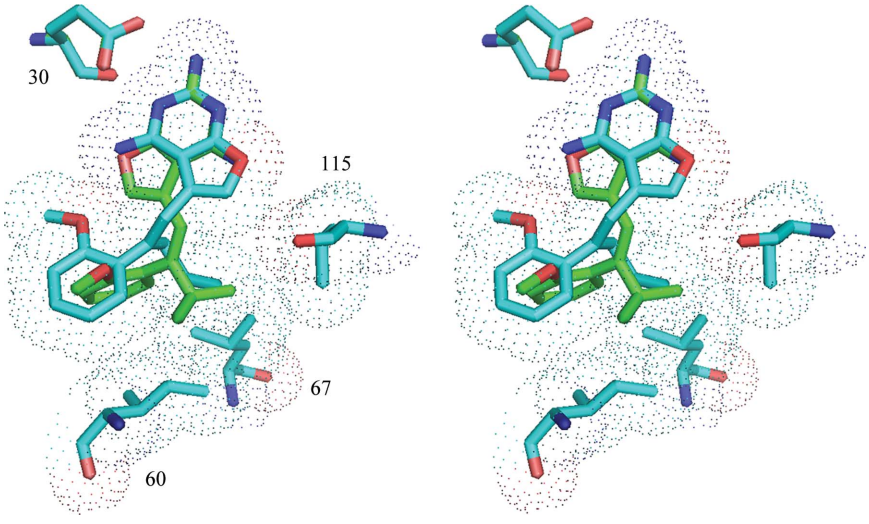

Figure 4
Superposition of *Z*3 (isopropyl; green) and *E*2 (propyl; cyan) in the active site of hDHFR highlighting the different modes of binding for the *E* and *Z* isomers of the furopyrimidine analogs. Also highlighted with van der Waals surfaces are the residues that make contact with the inhibitors: Ile60, Leu67 and Val115. Note that the C9-substituents occupy the same conformational space. This figure was generated with *PyMOL* (DeLano, 2002).

4. Discussion

The results of the structural analyses of the six 5-substituted 5-[2-(2-methoxyphenyl)-prop-1-en-1-yl]furo[2,3-*d*]pyrimidine-2,4-diamine analogs show that only one isomer of the chiral mixture of *E*/*Z* isomers present in the crystallization medium binds to hDHFR and furthermore that the *E* isomer is preferentially bound to hDHFR in five of the six analogs. Kinetic data for the resolved C9-methyl furopyrimidines showed that the *Z*1 isomer was the most potent against hDHFR, with a K_i of 0.5 μ*M* compared with 1.6 μ*M* for the *E* isomer (Gangjee *et al.*, 2009). The K_i for the 1:1 mixture of *E* and *Z* isomers for the C9-methyl inhibitor was also 0.5 μ*M*. Kinetic data for the mixed *E*/*Z* isomers presented here showed that the most potent analog was the 3:1 *E*:*Z* mixture for the isopropyl analog *Z*3 (Fig. 1), with a K_i of 0.83 μ*M* (Gangjee *et al.*, 2009). The structural data for this analog are consistent with these kinetic data in that the *Z* isomer also showed the most favorable intermolecular contacts for the isopropyl interactions with the hydrophobic residues Val115, Leu67, Ile60 and Thr56 (Table 3). Similarly, structural data show that the weakest inhibitor in this series, *E*6, binds with the isobutyl moiety disordered and makes less favorable intermolecular contacts (Table 3).

Previously reported structural data for the resolved C9-methyl *E*1 and *Z*1 analogs revealed that the *Z* isomer fitted the active site, while the *E* isomer could not easily be accommodated unless the 2,4-diaminofuropyrimidine ring were flipped such that Glu30 interacted with the 2-amino group and N3 of the pyrimidine ring and the furo oxygen occupied the N4 amino group

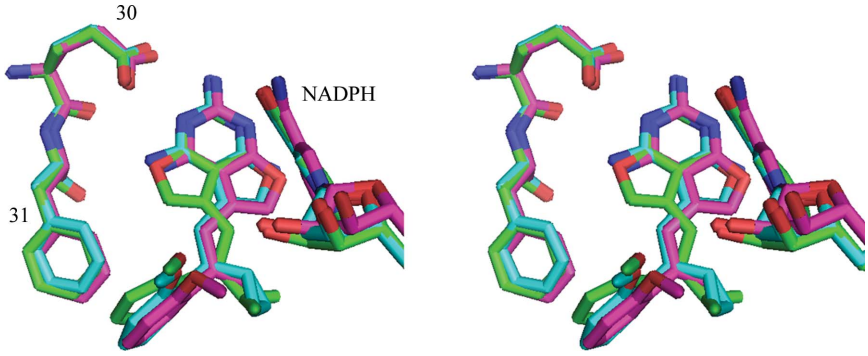

Figure 5
Stereo comparison of the binding of hDHFR with *Z*3 (green) and *E*4 (cyan) and of mouse DHFR with *E*1 (violet) in ternary complexes with NADPH. The active-site residues Glu30 and Phe31 are shown. Note that the 2′-methoxyphenyl ring binds in the same orientation in each of these complexes. This figure was drawn with *PyMOL* (DeLano, 2002).

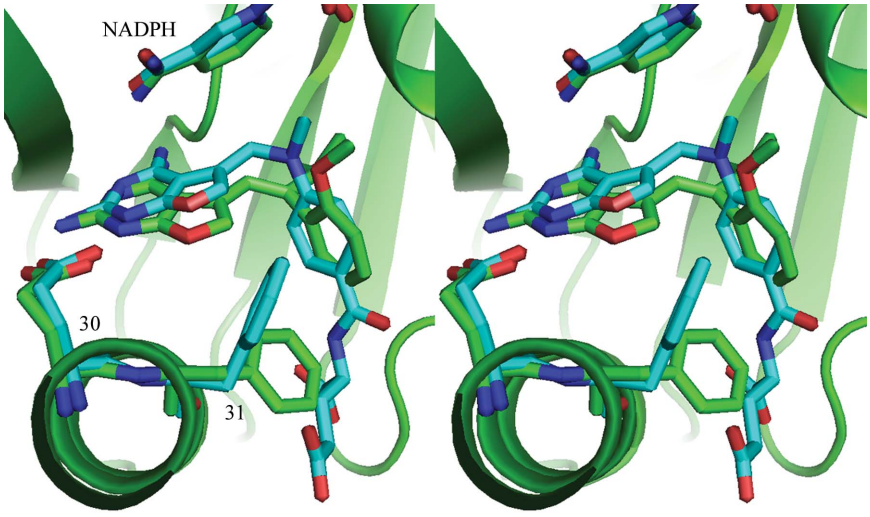

Figure 6
Stereoview of the binding of *Z*3 (isopropyl) to hDHFR (green) and that of the classical furopyrimidine MOT (PDB code 1hfr) to hDHFR (cyan) (Cody *et al.*, 1998). This figure was drawn with *PyMOL* (DeLano, 2002).

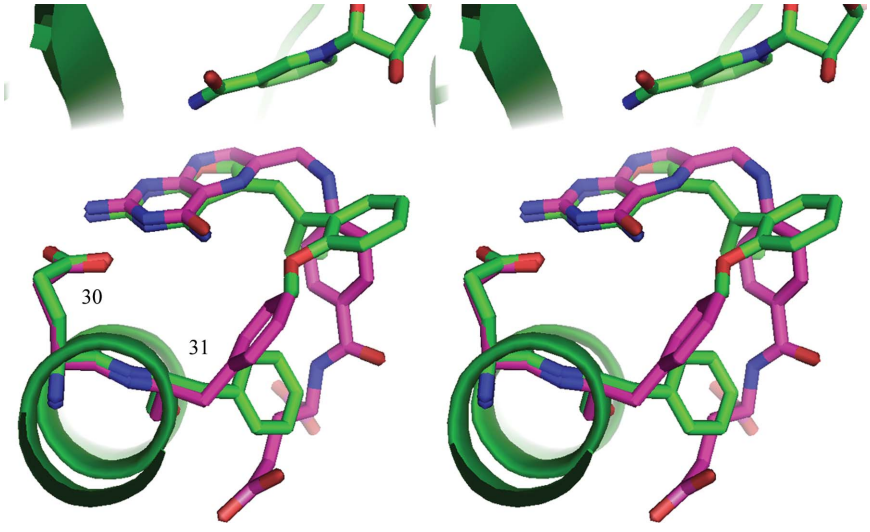

Figure 7
Steroview of *E*2 (C9-propyl) in hDHFR (green) and of folate in hDHFR (PDB code 1drf; Oefner *et al.*, 1988; violet). This figure was generated with *PyMOL* (DeLano, 2002).

position (Gangjee *et al.*, 2009; Cody *et al.*, 2009). The structures reported here indicate that the weaker binding analogs all bind as the *E*-isomer. Comparison of the binding of *Z* and *E* isomers reveals that the C9-propyl (*E*2) and C9-isopropyl (*Z*3) groups make hydrophobic contacts with the active-site residues Ile60, Leu67 and Val115 (Fig. 4, Table 3). In these structures, the 2,4-diaminofuro[2,3-*d*]pyrimidine ring of *E*2 is flipped with respect to that of *Z*3 and the 2′-methoxyphenyl ring of *E*2 is perpendicular to that of *Z*3 (Table 2, Fig. 4). Structural data for the *E*1 and *Z*1 complexes with mDHFR revealed that the 2′-methoxyphenyl rings had the same orientation, similar to that observed for the complexes of hDHFR with *Z*3 and *E*4 (Fig. 5).

In the *Z* isomer, the 2-amino group and N1 of the furopyrimidine ring interact *via* hydrogen bonds to Glu30, similar to the binding observed for antifolates such as methotrexate, trimethoprim and the classical furopyrimidine MOT (Fig. 6; Cody *et al.*, 1998). In this orientation, the 4-amino group of the *Z* isomer also makes a number of hydrogen-bonding interactions with the backbone functional groups of Ile7, Val115 and Tyr121 and the nicotinamide ring of NADPH (Cody & Schwalbe, 2006). On the other hand, the *E* isomer shows that the furopyrimidine ring is 'flipped' in the binding site such that the 2,4-diamino and N3 functional groups interact with Glu30, similar to that observed for the binding of folate (Cody & Schwalbe, 2006; Cody *et al.*, 1999; Oefner *et al.*, 1988). In this orientation, the 4-amino group occupies the 4-oxo group of folate (Fig. 7) and the furo oxygen occupies the position of the 4-amino group observed for the *Z* isomer.

These studies showed that hDHFR is able to preferentially bind specific isomers present in a mixture of *E* and *Z* isomers of these ligands. Although the active site can accommodate either isomer by flipping the orientation of the furopyrimidine ring, these data reveal that only one isomer is bound in any given complex. The mechanism for this selectivity is less clear, as both the *E* and the *Z* isomers can bind to the hDHFR enzyme. In this series of moderately potent furopyrimidine inhibitors, the majority of the analogs bound with what is likely to be the less potent isomer, as all but one complex shows binding of the *E* isomer. These observations may reflect binding with a

nonsaturating DHFR stoichiometry under the crystallization conditions within the crystal lattice.

The results of these structural studies reveal the flexibility observed in the binding of *E* and *Z* isomers of this series of furopyrimidines suggest that these analogs can serve as lead analogs for the development of more potent hDHFR inhibitors and that the conformational flexibility in binding of the *E* and *Z* isomers can provide novel templates for the design of more selective inhibitors of hDHFR.

This work was supported in part by grants from the National Institutes of Health GM51670 (VC) and CA09885 (AG).

References

Cody, V., Galitsky, N., Luft, J. R., Pangborn, W., Blakley, R. L. & Gangjee, A. (1998). *Anticancer Drug Des.* **13**, 307–315.
Cody, V., Galitsky, N., Rak, D., Luft, J. R., Pangborn, W. & Queener, S. F. (1999). *Biochemistry*, **38**, 4303–4312.
Cody, V., Luft, J. R. & Pangborn, W. (2005). *Acta Cryst.* D**61**, 147–155.
Cody, V., Pace, J., Lin, L. & Gangjee, A. (2009). *Acta Cryst.* F**65**, 762–766.
Cody, V. & Schwalbe, C. H. (2006). *Crystallogr. Rev.* **12**, 301–333.
Cohen, A. E., Ellis, P. J., Miller, M. D., Deacon, A. M. & Phizackerley, R. P. (2002). *J. Appl. Cryst.* **35**, 720-726.
Collaborative Computational Project, Number 4 (1994). *Acta Cryst.* D**50**, 760–763.
DeLano, W. L. (2002). *The PyMOL Molecular Viewer.* DeLano Scientific, Palo Alto, California, USA. http://www.pymol.org.
Emsley, P. & Cowtan, K. (2004). *Acta Cryst.* D**60**, 2126–2132.
Gangjee, A., Li, W., Lin, L., Zeng, Y., Ihnat, M., Warnke, L. A., Green, D. W., Cody, V., Pace, J. & Queener, S. F. (2009). *Bioorg. Med. Chem.* **17**, 7324–7336.
Gangjee, A., Zeng, Y., Ihnat, M., Warnke, L. A., Green, D. W., Kisliuk, R. L. & Lin, F.-T. (2005). *Bioorg. Med. Chem.* **13**, 5475–5491.
González, A., Moorhead, P., McPhillips, S. E., Song, J., Sharp, K., Taylor, J. R., Adams, P. D., Sauter, N. K. & Soltis, S. M. (2008). *J. Appl. Cryst.* **41**, 176–184.
Lovell, S. C., Davis, I. W., Arendell, W. B. III, de Baker, P. I. W., Word, J. M., Prisant, M. G., Richardson, J. S. & Richardson, D. C. (2002). *Proteins*, **50**, 437–450.
McPhillips, T. M., McPhillips, S. E., Chiu, H.-J., Cohen, A. E., Deacon, A. M., Ellis, P. J., Garman, E., Gonzalez, A., Sauter, N. K., Phizackerley, R. P., Soltis, S. M. & Kuhn, P. (2002). *J. Synchrotron Rad.* **9**, 401–406.
Oefner, C., D'Arcy, A. & Winkler, F. K. (1988). *Eur. J. Biochem.* **174**, 377–385.
Otwinowski, Z. & Minor, W. (1997). *Methods Enzymol.* **276**, 224–225.
Schüttelkopf, A. W. & van Aalten, D. M. F. (2004). *Acta Cryst.* D**60**, 1355–1363.